



Published in final edited form as:

Chem Biol Drug Des. 2014 December ; 84(6): 626–641. doi:10.1111/cbdd.12365.

Specific interaction between *Mycobacterium tuberculosis* lipoprotein-derived peptides and target cells inhibits mycobacterial entry *in vitro*

Marisol Ocampo^{1,2,3,*}, Hernando Curtidor^{1,2}, Magnolia Vanegas^{1,2}, Manuel Alfonso Patarroyo^{1,2}, and Manuel Elkin Patarroyo^{1,3}

¹ Fundación Instituto de Inmunología de Colombia (FIDIC), Carrera 50 No. 26–20, Bogotá, Colombia

² Universidad del Rosario, Carrera 24 No. 63C-69, Bogotá, Colombia

³ Universidad Nacional de Colombia, Carrera 45 No. 26-85, Bogotá, Colombia

Summary

Tuberculosis (TB) continues being one of the diseases having the greatest mortality rates around the world, 8.7 million cases having been reported in 2011. An efficient vaccine against TB having a great impact on public health is an urgent need. Usually, selecting antigens for vaccines has been based on proteins having immunogenic properties for patients suffering TB and having had promising results in mice and non-human primates. Our approach has been based on a functional approach involving the pathogen–host interaction in the search for antigens to be included in designing an efficient, minimal, subunit-based anti-tuberculosis vaccine. This means that *Mycobacterium tuberculosis* has mainly been involved in studies and that lipoproteins represent an important kind of protein on the cell envelope which can also contribute towards this pathogen's virulence. This study has assessed the expression of four lipoproteins from *M. tuberculosis* H37Rv, i.e. Rv1411c (LprG), Rv1911c (LppC), Rv2270 (LppN) and Rv3763 (LpqH), and the possible biological activity of peptides derived from these. Five peptides were found for these proteins which had high specific binding to both alveolar A549 epithelial cells and U937 monocyte-derived macrophages which were able to significantly inhibit mycobacterial entry to these cells *in vitro*.

Keywords

Synthetic peptide; *Mycobacterium tuberculosis*; high activity binding peptide (HAPB); multi-epitope vaccine; anti-tuberculosis vaccine.

* Corresponding author: Marisol Ocampo C. Cra. 50 No. 26-20 Bogotá, Colombia Tel:+57-1-3244672-3-4 ext 137. Fax: +57-1-4815269 mocampoc@unal.edu.co.

Conflict of interest
None declared.

Introduction

Tuberculosis (TB), caused by *Mycobacterium tuberculosis* (*Mtb*), is still a major cause of death around the world and a major public health problem, as shown by WHO statistics in 2011 showing an estimated 8.7 million new cases of TB (13% co-infected with HIV) and that 1.4 million people died from TB, including almost one million deaths amongst HIV-negative individuals and 430,000 amongst HIV-positive people (1). It is considered a global emergency due to the increased appearance of new highly-virulent (2) and drug-resistant strains (3, 4). An urgent public health need is thus to create new vaccines which can generate an efficient prophylactic effect or boost protective immunity in Bacillus Calmette-Guérin (BCG)-vaccinated individuals.

In vitro culturing of *Mtb* in the search for antigens having prophylactic or diagnostic potential has led to a complex set of proteins becoming recognised (culture filtrate proteins - CFP) whose main characteristic is their immunodominance. Some antigens have been involved in inducing a protective immune response or activating T-cells in infected humans and in animal models, thereby being considered good vaccine candidates. Biochemical approaches have identified such antigens as proteins which are abundantly secreted in culture medium, even though the functional characteristics of a very few of them have been analysed as invasion-mediators. It can be argued therefore, that in contrast to classical “vaccine-preventable” diseases, an effective vaccine against TB will have to elicit a response which is superior to natural immunity.

Some *Mtb* H37Rv characteristics should be highlighted, bearing in mind the importance of interactions between mycobacteria and host cells. This pathogen's envelop consists of the cell membrane, a cell wall and a layer similar to an external capsule. The mycobacterial cytoplasmic membrane has peculiar characteristics as the presence of some lipopolysaccharides which are also found in actinomycetales (5). This vital barrier provides osmotic protection and regulates specific solute traffic between the cytoplasm and the environment. Even though very little is known about the *Mtb* membrane, it has been stated that it contains many proteins which are important for the bacteria's physiology. Proteomic work has led to hundreds of such proteins being identified, including integral proteins having transmembrane domains and peripheral proteins on the membrane (6). Most of these proteins intervene in metabolic processes related to obtaining energy, degrading fatty acids and lipid synthesis, or in macromolecule metabolism; other proteins are involved in cell transport and division (7). Proteomic studies of the *Mtb* H37Rv membrane fraction have led to identifying some proteins responsible for this mycobacterium's pathogenicity (8). Different analytic techniques have identified a large amount of new proteins associated with the mycobacterial membrane (6) and new ORFs which have not been described to date for the *Mtb* genome (7). It has also been shown that mycobacterial membrane-associated proteins are potent T-cell response activators in humans (9, 10).

Bioinformatics represents a tool which has led to identifying 99 putative lipoproteins which are encoded in the *Mtb* genome (representing 2.5% of its proteome); this, in turn, has led to proposing that lipoproteins on the cell envelop could be contributing towards this pathogen's virulence (11). All bacteria apparently localise specific proteins on their cell envelops

through post-translational lipid modifications for producing membrane-anchored lipoproteins. Post-translational modifications are directed by the “lipobox” motif located at the C-terminal extreme of the signal sequence, consisting of four amino acids [LVI/ASTVI/GAS/C] located within the lipoprotein's signal peptide's sequence. Modifying mycobacteria involving lipids represents an important mechanism by which proteins become localised on the cell envelop and could possibly be virulence factors. Lipoprotein precursors are mainly translocated by a Sec-dependent pathway to the plasmatic membrane and then become modified on the cysteine residue (universally conserved and essential) located in the lipobox motif. Mycobacteria have an outer membrane-like structure around their cells (12, 13), the triacylated structure might play a role in lipoprotein translocation to the outer membrane in a manner similar to that seen in *E. coli*. However, the exact biological function of N-acylation in these species has not been determined (14). Lipoprotein biogenesis is dependent on the presence of specific type II signal peptide sequences. The signal peptide directs pre-prolipoprotein export through the plasma membrane whereupon a diacylglyceride unit is added by thioether linkage to a crucial cysteine residue. The enzyme that carries out this lipidation reaction (prolipoprotein diacylglyceryl transferase (Lgt)) is apparently an essential enzyme in Gram-negative bacteria but is dispensable in Gram-positive ones (11).

It has been reported (15) 33 of 42 lipoproteins identified by identified by LC MS/MS analysis using stringent database search criteria with a minimum of two peptides and an estimated FDR of less than 1%, in the culture filtrate indicating that they are secreted either by shedding (release of acylated lipoproteins) or shaving (proteolytic cleavage). Twenty-four of the proteins identified in the culture filtrate were also found in other fractions, predominantly cell wall and membrane. Lipoproteins LpqL, LppH, LppK, LppO, LprQ, ProX, SubI, thioredoxin and the conserved hypothetical threonine rich protein have been identified exclusively in the CFP. In contrast, lipoprotein GlnH, LppD, LpqD, LpqG, LprB, LprC, Mce1E and OppA have not been identified in the CFP. Other proteins, like the 19 kDa lipoprotein LpqH, a known glycoprotein, was identified with 2 peptides in the culture filtrate and 13 peptides in the membrane, indicating a specific enrichment of this lipoglycoprotein in the membrane fraction. Additional lipoproteins that were enriched in the membrane fraction include the SODC, lipoproteins LprA, LprG, LppX, and the periplasmic phosphate binding lipoprotein PSTS1 and PSTS2.

The lipopeptide-induced amplification of an MHC class II-restricted CD4⁺ T cell subset which unifies all major effector functions required for protection in human tuberculosis has also been reported. The strong immunogenicity of mycobacterial lipopeptides should be exploited for prophylactic and therapeutic immune intervention strategies against tuberculosis (16). However, little is known about the breadth of human T-cell responses to mycobacterial lipoproteins. A recent study has described *lspA* function as being required for T-cell activation. Because *lspA* catalyses signal peptide release from nascent prolipoproteins, polyclonal T-cells may be recognising signal peptide sequences as dominant antigens.

Diacylated lipoproteins bind the TLR2/TLR6 heterodimer, whereas triacylated lipoproteins bind the TLR1/TLR2 heterodimer. Previous studies have shown that the Rv1411c (LprG)

mycobacterial lipoprotein inhibits MHC class II Ag processing via a TLR2-mediated mechanism (17). However, it has been shown that MHC class II-dependent T-cell stimulation occurs despite TLR2 blocking, suggesting lipoproteins are heterogeneous in their effects on antigen processing. A significant body of literature supports the importance of *M. tuberculosis*-secreted protein antigens, and some have recently suggested that the strength of T-cell responses to these antigens may paradoxically assist this particular bacterium in its life-cycle (18).

The present article presents results obtained with peptides from two lipoproteins characterised in previous studies (Rv1411c/ LprG and Rv 3763 or LpqH/19kDa) and two lacking a defined function (LppC/Rv1911c and LppN/Rv2270). Lipoproteins such as Rv3763 have been widely studied; it is both cell wall-associated and secreted and is a candidate virulence factor. It acts by inducing apoptosis in differentiated THP-1 cells and monocyte-derived macrophages, such effect being both dose- and time-dependent; although it is a mycobacterial glycolipoprotein (based upon the use of recombinant p19 where the acylation signal had been removed), it has been concluded that its polypeptide component is responsible for signalling through TLR-2 and that the lipid moiety is not required (19).

Rv3763 has been described as a dominant adhesin, binding THP-1 monocytic cells via the macrophage mannose receptor (MR) and thus promoting mycobacterial uptake (20). *Mtb* lipoproteins Rv1411c and Rv3763 participate in regulating adaptive immunity by inducing cytokine secretion and co-stimulatory molecules in innate immune cells as well as through directly regulating memory T-lymphocyte activation (21).

Rv1411c is a 27 kDa secreted glycolipoprotein (22), with calculated molecular weight 24,6 kDa, although it has also been suggested that it is an integral membrane protein (23) which is exclusively present in the *Mtb* species complex. Rv1411c knockout has resulted in decreased *Mtb* virulence in mice and macrophages (24); likewise, Rv3763, nonacylated protein Rv1411c retains TLR2 activity (25).

A search for antigens which could be used in an anti-tuberculosis subunit vaccine based on synthetic and multi-antigen peptides emerging from previous studies (26, 27) has led to a robust, highly specific and sensitive methodology being proposed which could lead to identifying selected *Mtb* H37Rv protein sequences having high specific target cell binding ability, named high activity binding peptides (HABPs). They have inhibited bacilli entry in *in vitro* assays. Our approach has been based on promising findings regarding the development of a synthetic antimalarial vaccine (28) which has led to establishing a systematic methodology for identifying antigens for a synthetic, multi-epitope, minimum subunit-based vaccine. While recognizing the substantial differences between pathogens (for example, *Plasmodium falciparum* and *M. tuberculosis*), this methodology could be applied to different diseases caused by many infectious agents. Sequences having high specific target cell binding ability must be modified, when using such methodology, to improve their immunogenic and protection-inducing properties; one amino acid has to be replaced by another in the “critical” binding residues, in line with well-established criteria.

Many malaria studies concerned with different stages regarding infecting red blood cells or hepatocytes (29, 30) have revealed that HABPs are immunologically silent, do not induce any type of response and that they can become modified based on their structural characteristics, thereby increasing their immunomodulator ability and protection-inducing potential (i.e. against the bacillus).

Even when new methods have been implemented leading to evaluating candidate epitopes for a vaccine in animal models (31), the difficulties in testing antigens in a suitable model for tuberculosis cannot be ignored. All of the foregoing, forming part of a proposal for *in vitro* assays (32, 33) for evaluating the immunogenic characteristics of peptide sequences able to inhibit *M. tuberculosis* entry to different infection target cells, is a reasonable alternative for continuing studies of similar molecules to those reviewed here.

Materials and Methods

Bioinformatics analysis of Mtb lipoproteins

The proteins to be studied were selected using results obtained with bioinformatics tools: specific ones based on characteristics and subcellular localisation ones, as reported previously (34, 35).

A search was made for signal sequences for each transport route, selecting proteins based on their particular characteristics (Sec, Tat and “lipobox”) after analysing the *M. tuberculosis* H37Rv genome using available computational tools: SignalP 3.0 (<http://www.cbs.dtu.dk/services/SignalP/>), TatP 1.0 (<http://www.cbs.dtu.dk/services/TatP/>), LipoP 1.0 (<http://www.cbs.dtu.dk/services/LipoP/>).

Transmembrane and hydrophobicity topology was predicted for each protein to be selected using bioinformatics tool TMHMM (version 2.0) (<http://www.cbs.dtu.dk/services/TMHMM/>). Protein sequences were submitted to predictive analysis based on classification by overall subcellular localisation, using Gpos-PLoc (<http://www.csbio.sjtu.edu.cn/bioinf/Gpos/>), PSORTb v.2.0.4 (<http://www.psorth.org/psorth/>) and PA-SUB v.2.5 (<http://pasub.cs.ualberta.ca:8080/pa/Subcellular>) tools.

Once the proteins had been selected, BLink (“BLAST Link”) was used as an analytic tool for exploring similar protein sequences by accessing BLAST searches which had been precomputed for every protein sequence in the Entrez Protein data domain (<http://www.ncbi.nlm.nih.gov/sutils/blink.cgi?mode=query>), for comparing the sequences of lipoproteins LpqH, LprG, LppC and LppN in different *Mycobacterium* genus strains and species.

The presence of Mtb H37Rv lipoprotein-encoding genes

Chromosomal DNA extraction and PCR assay were used for corroborating the presence of genes encoding the proteins to be studied in the *M. tuberculosis* H37Rv (ATCC 27294), *M. tuberculosis* H37Ra (ATCC 25177), *M. bovis* (ATCC 19210) and *M. bovis* BCG (ATCC 27291, Pasteur substrain) strains in normal culture conditions and which were used for later studies. Briefly, all mycobacterial species and strains were grown for 5–15 d in Middlebrook

7H9 (Difco) supplemented with oleic acid, albumin, dextrose, NaCl (10% OADC) and incubated at their optimum temperature until cultures reached 0.5–1.0 OD₆₀₀. This should have provided a mid- to late-log phase culture; bacilli were harvested by spinning at 12,500 g for 20 min at 4°C, suspended in PBS and stored at –20°C.

Genomic DNA (gDNA) was isolated from mycobacteria using an Ultra Clean Microbial DNA Isolation Kit (MoBio Laboratories, Inc., Carlsbad, CA), following the manufacturer's instructions. The PCR assay was carried out in a LABNET MultiGene Thermal Cycler (Woodbridge, NJ, USA) by incubating 100 ng gDNA with a PCR mixture containing 1.25 units of BioTaqDNA polymerase (Bioline, London, UK), 1X Taq polymerase reaction buffer, 2.5 mM MgCl₂, 0.25mM dNTPs and 1 μM of each primer in a final 25-μL reaction volume. Extracted DNA quality was assessed by amplifying a 360 base pair fragment from the *rpoB* gene (encoding the B subunit of RNA polymerase) using the sense (5'-TCAAGGAGAAGCGCTACGA-3') and antisense (5'-GGATGTTGATCAGGGTCTGC-3') primers.

Four pairs of specific primers were used to assess the presence of the lipoprotein-encoding genes included in this study; the sequences for each primer were: *rv1411-D* (5'-ATGCGGACCCCCAGACG-3') and *rv1411-R* (5'-GTGACCTGGACCTTCTCG-3'); *rv1911-D* (5'-CGGTGACAGTCGAGAGAC-3') and *rv1911-R* (5'-CCTGTGCTATCGCCTGTG-3'); *rv2270-D* (5'-CGTGCGGCATTGCGTC-3') and *rv2270-R* (5'-GCAGCAAACAGATGACGG-3'); *rv3763-D* (5'-GTCGACTACAGGAAGCGG-3') and *rv3763-R* (5'-GCGGTCCCAGTGATCTTG-3').

The reaction was carried out under the following conditions: an initial denaturing step at 95°C for 5 min followed by 35 cycles consisting of: 1 min at 56°C (for *rv1411* and *rv1911*) or at 58°C (for *rv2270* and *rv3763*), 1 min at 72°C and 1 min at 95°C. A final extension cycle at 72°C for 5 min was performed. Nuclease-free water was included in each assay as negative control, using the same reaction conditions. The amplified products were visualised on 2% agarose gels stained with SYBR Safe (Invitrogen, Carlsbad, CA)

Polyclonal antibody recognition of lipoproteins

The expression of proteins of interest was corroborated, bearing in mind the molecular weights of the bands recognised by polyclonal sera obtained by inoculating polymer peptides from such proteins of interest. The polymer peptide sequences for each lipoprotein were Rv1411c-CG³¹SKPSGGPLPDAKPLVEEATAQT⁵²GC, Rv1911c-CG¹²⁵SGSTADGQTPAGGHSVPNSG¹⁴⁴GC, Rv2270-CG²³SNGARGGIASSTNMNPTNPPA⁴²GC and CG⁴³TAETATVSPPTAPQSARTET⁶²GC and Rv3763-CG⁸⁶AAVLTDGNPPEVKSVGLGNV¹⁰⁵GC.

The lipoprotein peptide sequences chosen for immunising rabbits were obtained using BepiPred 1.0b Server epitope prediction software, available at <http://www.cbs.dtu.dk/services/BepiPred/> (36). New Zealand rabbits (previously determined as being non-reactive to *Mtb* sonicate by Western blot) were inoculated with 0.5 mg polymerised peptide. These polymers were emulsified with Freund's incomplete adjuvant (FIA) and administered on

days 0, 20, and 40. Bleeding was carried out 20 d after the third inoculation and polyclonal antibodies were obtained for protein immunodetection.

Mtb H37Rv proteins from total sonicate and different cell fractions (wall, membrane and cytosol, obtained through the National Institute of Health (NIH) Biodefense and Emerging Infection Research Resources Repository, National Institute of Allergy and Infectious Diseases (NIAID)), were separated in a SDS-PAGE discontinuous system, using a 10% to 20% polyacrylamide gradient. A total of 1 mg/mL from each fraction and sonicate were loaded onto each gel. The gels were transferred to nitrocellulose membranes, using the semi-dry blotting technique (37), which were then blocked (locking solution: 1% TBS-Tween and 5% milk). Membranes were incubated for one hour with a 1:100 dilution from each rabbit serum obtained. After $5 \times 1\%$ TBS-Tween washes, they were incubated for one hour with a 1:5,000 dilution of alkaline phosphatase conjugated with anti-rabbit IgG antibody. Reactions were revealed with NBT/BCIP.

Electro-immune microscopy represents another approach to lipoprotein subcellular localisation; fine cuts (400 nm) of mycobacteria immersed in LR White resin were thus prepared. The same immunoblot sera were used as primary antibody and anti-rabbit IgG, coupled to colloidal gold particles, was used as secondary antibody; 6% uranyl acetate was added to provide contrast for the samples. Localisation was determined by using a Hitachi Hu-12A transmission electron microscope.

Interaction between synthetic lipoprotein peptides and target cells

Receptor-ligand type *in vitro* assays were used for determining sequences regarding specific binding to cell lines which could have been possible targets for infection by *Mtb* H37Rv (i.e. A549 alveolar epithelial cells and U937 human monocyte-derived macrophages).

U937 cells (2×10^5 /ml, ATCC CRL-1593.2) were differentiated using 200 nM phorbol 12-myristate 13-acetate (PMA, Sigma-Aldrich) for 3 days to become adherent. A549 (ATCC CLL-185) cells were grown in RPMI 1640 medium (Gibco) supplemented with 10% heat-inactivated foetal bovine serum and kept at 37°C in 5% CO₂. Both adherent cell lines were dislodged by suspension in 1X non-enzymatic cell dissociation solution (NECDS) (Sigma) for 3 min at 37°C and collected by spinning at 500g for 5 min. The pellet was suspended in non-supplemented RPMI 1640 medium until further use.

Synthetic peptides covering selected protein's complete sequences were used; they were radiolabelled and incubated with target cells. Briefly, 1.5×10^6 cells were incubated with different concentrations of radiolabelled peptide (0 to 950 nM), in the presence (non-specific binding) or absence (total binding) of the same non-radiolabelled peptide (40 μM), for 90 minutes at 4°C. An aliquot of this mixture was passed through a 60:40 dioctylphthalatedibutylphthalate cushion (1,015 g/mL) and centrifuged at 4,500 g for 3 minutes. A gamma counter was used for quantifying cell-associated radioactivity. All assays were performed in triplicate. Specific binding values were obtained by subtracting non-specific binding from total binding values; specific binding for each cell line was calculated from the specific binding curve slope. Peptides having greater than 1% specific binding

were considered high activity binding peptides (HABPs). These parameters had already been established from previous studies in our laboratory (26, 27).

Saturation assays were carried out for characterising HABP target cell binding. 1.5×10^6 A549 cells or 1.5×10^6 U937 cells were incubated with increasing (0–7000 nM) radio-labelled HABP concentrations in the presence or absence of 30 μ M unlabelled HABP. Following incubation, unbound peptide was removed from cells by sedimentation through a dioctylphthalate–dibutylphthalate cushion ($d = 1.015$ g/ml). The curves so obtained were analysed by saturation and Hill analysis.

HABP secondary structure

Each lipoprotein peptide's secondary structure elements were studied by circular dichroism (CD). Peptides were dissolved in 30% trifluoroethanol (TFE) in water and the spectrum was acquired at 20°C by averaging three scans taken on a Jasco J-810 spectropolarimeter, using a 1.00-cm pathway cuvette (Jasco Inc, Easton, MD). This was corrected for baseline subtraction (260–190 nm wavelength range, 20 nm/min scan rate, 1 nm bandwidth) (38).

The results were expressed as mean residue ellipticity $[\Theta]$, units being degrees \times cm² \times dmol, according to $[\Theta] = \Theta\lambda / (100lc)$, where $\Theta\lambda$ was measured ellipticity, l was optical path length, c peptide concentration and n the number of amino acid residues in a particular peptide sequence.

Inhibiting Mtb H37Rv entry in vitro

Once peptides having high specific target cell binding ability had been selected, it was determined whether they could inhibit the entry of *Mycobacterium tuberculosis* H37Rv which had already been labelled with SYBR safe according to previously reported *in vitro* assay, conditions using a flow-cytometry-based assay (39, 40). Briefly, A549 and U937 cells (2.5×10^5 per well), adhered in 24-well plates overnight, were then incubated with different peptide concentrations (2 μ M, 20 μ M and 200 μ M) for 2 hours. SYBR-safe-stained mycobacteria (2.5×10^7) suspended in RPMI medium were added to each well (1:100 MOI) and incubated overnight at 37°C. Inhibition control consisted of 10 μ M cytochalasin D. Extracellular bacilli were removed by washing with HBSS and cells were dislodged from monolayers and fixed with 4% p-formaldehyde. The samples were stained with methylene blue for FACScan flow cytometry analysis (Becton Dickinson); 5,000 events were collected for determining the percentage of SYBR-safe positive corresponding to infected cells detected on the FL1 channel. Data was statistically analysed using a Student's t-test.

HABPs' cytotoxic effect was evaluated using rezasurine (*in vitro* toxicology assay kit, Sigma), following the manufacturer's recommendations. Briefly, cell cultures were removed from incubator, rezasurine dye solution was added in an amount equal to 10% of the culture medium volume; cultures were then returned to an incubator for 2 h. Samples were measured fluorometrically by monitoring the increase in fluorescence at 590 nm wavelength, using a 560 nm excitation wavelength.

Internalising microspheres into target cells in the presence of HABPs

An internalisation assay, involving A549 cell uptake of fluoresbrite carboxylate GY fluorescent microspheres (1.0 Micron Microspheres from Polysciences, Inc), was based on the procedure described by El-Shazly (41); it was standardised by our group, following the manufacturer's instructions. Briefly, GY microspheres (2.5×10^6) were coated with the chosen peptides (at 2, 20 and $200 \mu\text{M}$) by incubation in PBS1X at 37°C for 1 h and then suspended in incomplete RPMI medium. Peptide-coated microspheres and 2.5×10^5 A549 cells (previously adhered to 24-well plates overnight) were incubated for 1 h at 37°C , MOI 1:10 cell-microspheres. The supernatant was removed and the cells were washed thrice with Hank's balanced salt solution (HBSS) to eliminate extracellular microspheres and then detached using 0.3% trypsin and 0.017mM EDTA solution. Cells were spun at 2,500 rpm for 10min and suspended in $200 \mu\text{L}$ PBS for reading by flow cytometry. 5,000 events were collected for determining the FITC positive percentage of internalised microspheres detected on the FL1 channel.

As control for differentiating peptide effect on these cells, 2.5×10^5 A549 adhered cells were incubated with peptides (2, 20 and $200 \mu\text{M}$) and GY microspheres (2.5×10^6) were then added without peptide. It was thus possible to determine whether microsphere internalisation was induced by coating GY microspheres with peptide or by peptide action alone. GY microspheres without peptide were also incubated with A549 adhered cells as negative control. Counting in a Neubauer chamber in Trypan blue-stained 1:1 dilution using fluorescence microscopy was used for confirming that flow cytometry count really accounted for internalised microspheres.

Results

Bioinformatics analysis of Mtb lipoproteins

Rv 1411c, Rv1911c, Rv2270 and Rv3763 lipoproteins were selected, according to the results obtained from *Mtb* H37Rv genome sequence analysis (Table 1). The selected proteins had low molecular weight ($\sim 20\text{kDa}$), thereby leading to later studies aimed at elucidating their 3D structure by using nuclear magnetic resonance in our laboratory. Both Rv1411c and Rv3763 have been studied by other authors; their *Mtb* membrane proteomic studies (6, 8) led to finding that they were immunogenic and could modulate an immune response by binding to Toll-like receptor-2 (25, 42, 43). Rv1911c and Rv2270 lipoproteins do not have a known function; however, their characteristics regarding topology and secretion route suggest that they could be anchored to mycobacterial surface and involved in interaction with infection target cells.

Multiple alignment of the sequences reported for each selected lipoprotein showed that LpqH, LprG, LppC and LppN were conserved in *M. tuberculosis* complex (MTBC) strains and species. It was also observed that the selected lipoproteins' sequences were present in different *Mtb* clinical isolates. Some variations were found in non-MTBC mycobacteria lipoprotein sequences. The MTC's importance lies in its grouping species having great medical and veterinary importance, such as *M. tuberculosis* H37Rv, *M. tuberculosis* H37Ra, *M. bovis*, *M. bovis* BCG, *M. africanum* and *M. microti* causing human and animal

tuberculosis, and identifying proteins present in CMT species but not in mycobacteria which are saprophytic for human beings. This could have great relevance in the search for sequences which some mycobacteria require in relation to their pathogenicity.

Mtb lipoprotein presence and expression

PCR experiments were run with mycobacterial gDNA for confirming the presence of the lipoproteins of interest in the *Mtb* H37Rv laboratory reference and *Mtb* H37Ra, *M. bovis* and *M. bovis* BCG strains in normal culture conditions. PCR experiments showed a good DNA mycobacterial quality as the *rpoB* gen was obtained as a 360 bp amplification fragment in mycobacterial strains (Figure 1A).

The presence of the *rv1411*, *rv1911*, *rv2270* and *rv3763* genes was confirmed in these strains; 692, 479, 406 and 330 base pairs (bp) amplification fragments were obtained for each gene, respectively (Fig 1B). The *rpoB* gene was obtained as a 360 bp amplification fragment in *Mtb* H37Rv.

The expression of proteins of interest was analysed bearing in mind the molecular weights of the bands recognised by polyclonal sera obtained by inoculating polymer peptides from such proteins. The first panel of Figure 2A (total sonicate) shows recognition of some bands between 15kDa and 30kDa, ~21kDa and ~18kDa predominating, where lipoproteins Rv1411c, Rv1911c, Rv2270 and Rv3763 could probably be found according to the reported ranges of theoretical molecular weights (Table 1). Strongly recognised proteins were Rv1411c and Rv3763, whereas the polyclonal antibodies weakly recognised proteins Rv1911c and Rv2270, in both complete sonicate and membrane fractions. All of them were weakly recognised in cell wall fraction but not in cytosol fraction.

Lipoprotein localisation was corroborated by IEM. Figure 2 B shows that such lipoproteins were surface proteins due to the presence of more colloidal gold particles on *Mtb* H37Rv surface than inside the bacillus. Rv1911c and Rv2270 protein particles were located on the surface in the more peripheral region, while particles were on the surface's inner region for the other two proteins. Later assays must confirm the presence, expression and localisation of the proteins of interest in the laboratory strain in normal growth conditions.

The interaction between Mtb lipoproteins and target cells

Taking lipoprotein localisation into account, 20 amino acid non-overlapped peptides covering the whole proteins sequence were synthesised. The binding assay was done at four different ¹²⁵I-radio-labelled peptide concentrations in the presence or absence of at least 100 times excess unlabelled peptide. Two curves were obtained in this assay: total binding and non-specific binding curves (Fig. 3, left panel). The specific binding curve resulted from subtracting non-specific binding from total binding (Fig. 3, right panel). Binding activity was defined as being the slope of the specific binding curve in the added peptide range. Binding assays allowed specific cell binding activity curves to be obtained for the forty peptides from the four lipoproteins where three different types of behaviour were observed: peptides having high specific binding activity, those presenting nonspecific binding activity and peptides having no binding activity at all. Peptides such as Rv1911c 37768

(¹⁰¹LVVDDPDAVGGLYVHWIVTG¹²⁰) had high specific A549 cell binding activity (radiolabelled peptide binding was inhibited by the same unlabelled peptide), while peptides like 37769 (¹²¹IAPGSGSTADGQTPAGGHSVY¹⁴⁰) had high nonspecific U937 cell binding activity (this bound to cells but there was no inhibition with the same non-radiolabelled peptide). Peptides such as 37770 (¹⁴¹PNSGGRQGYFGPCPPAGTGT¹⁶⁰) did not have A549 cell binding activity.

Figure 4 gives the ligand-receptor type assay results (i.e. the profile for each protein peptides' binding to U937 and A549 cells); the black bars represent the binding percentage. Eight HABPs were identified for Rv1411c: 37088 (²¹ATVVAGCSSGSKPSGGPLPDY⁴⁰), 37091 (⁸¹TTNPTAATGNVKLTLGGSDIY¹⁰⁰), 37093 (¹²¹SDFGPAADIYDPAQVLNPDY¹⁴⁰), 37094 (¹⁴¹GLANVLANFADAKAEGRDTIY¹⁶⁰), 37095 (¹⁶¹NGQNTIRISGKVSQAQAVNQIY¹⁸⁰), 37096 (¹⁸¹APPFNATQPVPATVWQIETGY²⁰⁰), 37097 (²⁰¹DHQLAQAQLDRGSGNSVQMTY²²⁰) and 37098 (²¹⁸QMTLSKWGEKVQVTKPPVSY²³⁶). 37094 and 37098 had high binding to both cell lines, possibly recognising a common receptor on cell surface; however, further studies are needed for establishing these HABPs' receptors on target cells. Seven HABPs were found for Rv1911c: 37763 (¹MESPMTSTLHRTPLATAGLAY²⁰), 37764 (²¹LVVALGGCGGGGDSRETPPY⁴⁰), 37765 (⁴¹YVPKATTVDATTPAPAAEPL⁶⁰), 37766 (⁶¹TIASPMFADGAPIPVQFSCY⁸⁰), 37767 (⁸¹GANVAPPLTWSSPAGAAELAY¹⁰⁰), 37768 (¹⁰¹LVVDDPDAVGGLYVHWIVTG¹²⁰) and 37769 (¹²¹IAPGSGSTADGQTPAGGHSVY¹⁴⁰). 37763 and 37768 had high specific binding to both cell lines. Four peptides were HABPs in the Rv2270 protein: 37775 (²¹CSSNGARGGIASSTNMNPTNPY⁴⁰), 37777 (⁶¹ETWINLQVGDCLADLPPADLY⁸⁰), 37779 (¹⁰¹RAPVAVDAAVSMANRDCAAY¹²⁰) and 37780 (¹²¹GFAPYTGQSVDTSPYSVAYL¹⁴⁰). The last two were able to bind in a highly specific manner to both cell lines. Only Rv3763 37070 (⁴¹TASPGAASGPKVVIDGKDQNY⁶⁰) was a U937 cell HBP; no peptide had high specific A495 cell binding in this protein.

Saturation assays were carried out with those having high specific binding for characterising their interaction with cells; thus Rv1411c 37094, Rv1911c 37768, Rv2270 37779 were used with U937 and A549 cells and Rv3763 37075 only with U937 cells (Figure 5). Saturation curves and Hill analysis were performed and dissociation constants (K_D) between 800, and 2,600 nM were obtained for these HABPs. Hill coefficients (nH) greater than 1.0 were obtained for HABPs, suggesting positive cooperativity for these ligand-receptor interactions, thereby suggesting that a first ligand molecule's binding to its receptor facilitated the binding of the following molecule from the same ligand; the number of receptors for these HABPs on U937 or A549 cells was calculated for these HABPs (Table 2).

Once HABPs had been identified for each protein of interest, it was necessary to establish whether such sequences could inhibit *Mtb* H37Rv entry to target cells in *in vitro* assays. Inhibition assay results could have suggested some function for such proteins.

Determining HABP inhibition ability

Once peptides having high specific target cell binding ability had been selected, it was determined whether they could inhibit the entry of *Mycobacterium tuberculosis* H37Rv which had already been labelled with SYBR safe, according to previously reported *in vitro* assay conditions (40). The ability to inhibit mycobacterial entry to target cells was defined as being the difference between the amount of mycobacteria internalised by a cell in the absence of inhibitors (100% of invasion) and mycobacteria internalised in the presence of 2 μ M, 20 μ M or 200 μ M HABP concentrations; 10 μ M cytochalasin D (SIGMA, St. Louis, MO) was used as invasion inhibitor (i.e. negative control).

Samples were quantified using a FACScan cytometer (Becton Dickinson); the graphs are shown in the upper part of Figure 6. Data was obtained and analysed using Cellquest software (Becton Dickinson). Uninfected epithelial cells were discriminated from infected epithelial cells according to light FL1 characteristics. Figure 6 shows that HABPs such as Rv1411c 37091 and 37094, Rv1911c 37763, 37767, 37768 and 37769, Rv 2270 37779 and 37780 and Rv3763 37070 significantly inhibited *Mtb* H37Rv entry to U937 cells. Entry to A549 cells was inhibited by the presence of HABP Rv1411c 37088, 37094, 37096, 37097 and 37098, Rv1911c 37764, 37767 and 37768 and Rv2270 37775, 37779 and 37780.

However, it was also observed that some peptides which did not have specific target cell binding weakly inhibited mycobacterial entry (<10%). HABPs having inhibitory activity in both cell lines are of interest in continuing the proposed methodological design (i.e. 37094, 37767, 37768, 37779, 37780). Scrambled HABPs (having the same amino acid composition but different sequence) were synthesised and their inhibitory activities were also determined by following the same methodology, less than 10% inhibition values being obtained.

Cytotoxicity assay results demonstrated that none of the HABPs assessed at different concentrations had cytotoxic effects on cells, maintaining viability levels comparable to those obtained for control cells (cells only incubated with RPMI). None of the assessed treatments showed differences regarding this control.

A549 cell internalisation of HABP-coated microspheres

Previous studies have shown the usefulness of using fluorescent protein-coated latex beads to study *Mtb* protein uptake and internalisation by non-phagocytic cells (HeLa cells) (41, 44); hence, this study was aimed at determining whether microspheres coated with purified synthetic peptides from selected lipoproteins were internalised by A549 cells. Sixteen peptides were analysed in internalisation assays, finding a ~12% maximum internalisation peak for HABP 37766 (Rv1911c), as shown in Figure 7. A modified internalisation assay (control treatment) consisting of directly incubating cells with peptide and then adding microspheres was carried out to differentiate the peptide's effect on these cells, i.e. to determine whether microsphere internalisation was induced by peptide coating the latex beads or by peptide action alone. As can be observed in Fig. 7, HABPs 37088, 37098, 37766 and 37767 caused significant microsphere internalisation, whereas control treatment internalisation percentage was always lower than the percentages obtained with peptide-

coated beads. Not all HABPs induced significant microsphere internalisation, suggesting that only some HAPB proteins may play important roles during cell invasion.

HAPB structural elements

Bearing in mind the relationship between peptide structure and function as a ligand, structural element content had to be determined by circular dichroism (CD) analysis for all peptides from the proteins being studied. Spectra obtained for HABPs are shown in supplementary Figure 1; it can be seen that most HABPs had α -helix structural elements, characterised by a 212 nm maximum and 207 and 222 nm minima, while HABPs such as 37098, 37764 or 37777 had a random coil configuration, characterised by a 198 nm minimum and 212 nm maximum. SELCON, CONTINLL and CDSSTR deconvolution software (38, 45) was used for the corresponding analysis. A conformational–functional correlation between HABPs could not be determined.

Discussion

Whilst most approaches in the search for antigens for an anti-tuberculosis vaccine have been based on finding T-epitopes recognised by individuals suffering active or latent disease, our group has adopted a fresh approach based on a logical and rational methodology leading to identifying important antigens involved in the pathogen-host interaction (i.e. a functional approach) (26, 27).

This article was aimed at dealing with the aforementioned approach involving *Mtb* H37Rv lipoprotein Rv1411c, Rv1911c, Rv2270 and Rv3763 peptides arousing special interest due to their topological characteristics. It has been described that the Rv3763 protein (19-kDa antigen) binds THP-1 monocyte cells via the macrophage mannose receptor (MR) thereby promoting uptake (20); however, this is the first report regarding a sequence from this protein binding to U937 monocyte-derived macrophages. Future studies must be aimed at determining whether this protein binds to U937 cells and whether HAPB 37070 (41 TASPGAASGPKVVIDGKDQNY 60) can inhibit such binding.

Immunogenic properties have been described for both Rv3763 and Rv1411c, but they have not been functionally characterised regarding their ability to interact with cells which are the target for infection. No reports regarding Rv1911c and Rv2270 were found in the pertinent literature. This report was thus aimed at ascertaining that genes encoding the four proteins of interest were present in some *Mycobacterium tuberculosis* complex strains and that the proteins were located on *Mtb* H37Rv surface, in normal culture conditions; this position should be favourable for interaction with target cells. Even though the molecular weight of the bands detected by immunoblotting was variable regarding their theoretical weight, the lipid or glycoside modifications presented by such proteins could have influenced these variations; proteomic studies have detected Rv1411c and Rv3763 proteins in the cell wall and having spots of low intensity. 2-D electrophoresis has also revealed many spots in the 20–40kDa region which have not been identified to date. There may have been low percentages of many functionally important proteins, meaning that they could not be detected (46). Regarding protein peptide interaction with U937 monocyte-derived macrophages, it was found that whilst Rv3763 only had one peptide having high specific

binding to these cells, the others had 3 to 4 HABPs distributed throughout such protein sequences. Concerning A549 cell binding, Rv3763 had no HABPs, suggesting that this protein does not interact with epithelial cells, only with monocyte cell lines (U937 and THP-1(20)). Rv1411c and Rv1911c binding regions were found at the C-terminal (37093–37098) and N-terminal extreme (37763–37768), respectively. Sequences having high binding ability to both cell lines (the target for infection) assayed here were of special interest, i.e. 37094, 37098, 37763 (corresponding to the signal sequence), 37767, 37768, 37779 and 37780. HABPs which inhibited *Mtb* H37Rv entry to U937 monocyte and A549 epithelial cells (Rv1411c 37094, Rv1911c 37767 and Rv2270 37768, 37779 and 37780) were taken into account for further studies concerning their immunogenic properties to consider whether to include them in our vaccine approach. HABP 37767 promoted epithelial cell entry to microspheres, suggesting an important role in interaction with A549 cells which are the target for infection.

Concerning the Rv3763 protein, bearing pathogen-host cell interaction in mind, only one sequence was relevant (HABP 37070) for monocyte cells; this showed that an immunogenic sequence may not be important for an interaction with the infection target cell and thus it is proposed that sequences having high binding capacity should be modified so that they can be recognised from an immunological point of view. Further studies are thus needed for determining the sequences' antigenic or immunogenic properties and, according to what has been proposed by other models, modifications to sequences may be required concerning such sequences' structure to allow them to become included in designing a minimal subunit-based, multi-epitope, chemically-synthesised anti-tuberculosis vaccine.

A common structural characteristic could not be established for peptides having high specific binding and mycobacterial entry inhibition ability. However, structural characterisation of the peptides of interest led to modifying them, bearing in mind that previous studies (28, 47) have shown that conserved HABPs having an α -helical structure tend to bind to MHC class II HLADR52 molecules whilst those having random or β -turn type structure tend to bind to HLA-DR 53 molecules. Secondary structure is thus critical in determining preferential MHC-peptide-TCR-complex activation.

Bioinformatics prediction tools (48) have been used for comparing HABP sequences to those for T-epitopes for *M. tuberculosis* lipoproteins Rv1411c, Rv1911c, Rv2270 and Rv3763. It was found that sequences predicted as being T-epitopes did not correspond to the sequences for high capacity binding peptides; only peptides 37763 and 37764 (HABPs) contained a sequence (HRTPLATAGLALVVALGGCG) predicted as being a T-epitope. Even though studies for experimentally determining HABP immunogenicity are only just getting under way, our previous experience leads to expecting that that these sequences must be modified to make them immunologically significant (28).

Supplementary Material

Refer to Web version on PubMed Central for supplementary material.

Acknowledgments

We would like to thank Jason Garry for translating and reviewing this manuscript. The *Mtb* H37Rv subcellular protein fractions were obtained through the National Institute of Health (NIH) Biodefense and Emerging Infection Research Resources Repository, National Institute of Allergy and Infectious Diseases (NIAID).

References

1. WHO. Global tuberculosis report 2012. World Health Organization; Geneva: 2012. Global tuberculosis report 2012..
2. Marquina-Castillo B, Garcia-Garcia L, Ponce-de-Leon A, Jimenez-Corona ME, Bobadilla-Del Valle M, Cano-Arellano B, et al. Virulence, immunopathology and transmissibility of selected strains of *Mycobacterium tuberculosis* in a murine model. *Immunology*. 2009; 128:123–33. [PubMed: 19191912]
3. Mlambo CK, Warren RM, Poswa X, Victor TC, Duse AG, Marais E. Genotypic diversity of extensively drug-resistant tuberculosis (XDR-TB) in South Africa. *Int J Tuberc Lung Dis*. 2008; 12:99–104. [PubMed: 18173885]
4. Engstrom A, Morcillo N, Imperiale B, Hoffner SE, Jureen P. Detection of first- and second-line drug resistance in *Mycobacterium tuberculosis* clinical isolates by pyrosequencing. *J Clin Microbiol*. 2012; 50:2026–33. [PubMed: 22461677]
5. Mahapatra, S.; Bau, J.; Brennan, P., et al. Structure, biosynthesis, and genetics of the Mycolic Acid-Arabinogalactan-Peptidoglycan complex.. In: Press, A., editor. Structure, biosynthesis, and genetics of the Mycolic Acid-Arabinogalactan-Peptidoglycan complex. Washington DC: 2005. p. 275-85.
6. Gu S, Chen J, Dobos KM, Bradbury EM, Belisle JT, Chen X. Comprehensive proteomic profiling of the membrane constituents of a *Mycobacterium tuberculosis* strain. *Mol Cell Proteomics*. 2003; 2:1284–96. [PubMed: 14532352]
7. Cole ST, Brosch R, Parkhill J, Garnier T, Churcher C, Harris D, et al. Deciphering the biology of *Mycobacterium tuberculosis* from the complete genome sequence. *Nature*. 1998; 393:537–44. [PubMed: 9634230]
8. Sinha S, Arora S, Kosalai K, Namane A, Pym AS, Cole ST. Proteome analysis of the plasma membrane of mycobacterium tuberculosis. *Comparative and functional genomics*. 2002; 3:470–83. [PubMed: 18629250]
9. Sinha S, Kosalai K, Arora S, Namane A, Sharma P, Gaikwad AN, et al. Immunogenic membrane-associated proteins of *Mycobacterium tuberculosis* revealed by proteomics. *Microbiology*. 2005; 151:2411–9. [PubMed: 16000731]
10. Mehrotra J, Bisht D, Tiwari VD, Sinha S. Serological distinction of integral plasma membrane proteins as a class of mycobacterial antigens and their relevance for human T cell activation. *Clin Exp Immunol*. 1995; 102:626–34. [PubMed: 8536383]
11. Sutcliffe IC, Harrington DJ. Lipoproteins of *Mycobacterium tuberculosis*: an abundant and functionally diverse class of cell envelope components. *FEMS microbiology reviews*. 2004; 28:645–59. [PubMed: 15539077]
12. Hoffmann C, Leis A, Niederweis M, Plitzko JM, Engelhardt H. Disclosure of the mycobacterial outer membrane: cryo-electron tomography and vitreous sections reveal the lipid bilayer structure. *Proc Natl Acad Sci U S A*. 2008; 105:3963–7. [PubMed: 18316738]
13. Zuber B, Chami M, Houssin C, Dubochet J, Griffiths G, Daffe M. Direct visualization of the outer membrane of mycobacteria and corynebacteria in their native state. *J Bacteriol*. 2008; 190:5672–80. [PubMed: 18567661]
14. Nakayama H, Kurokawa K, Lee BL. Lipoproteins in bacteria: structures and biosynthetic pathways. *The FEBS journal*. 2012; 279:4247–68. [PubMed: 23094979]
15. Bell C, Smith GT, Sweredoski MJ, Hess S. Characterization of the *Mycobacterium tuberculosis* proteome by liquid chromatography mass spectrometry-based proteomics techniques: a comprehensive resource for tuberculosis research. *Journal of proteome research*. 2012; 11:119–30. [PubMed: 22053987]

16. Bastian M, Braun T, Bruns H, Rollinghoff M, Stenger S. Mycobacterial lipopeptides elicit CD4+ CTLs in *Mycobacterium tuberculosis*-infected humans. *J Immunol.* 2008; 180:3436–46. [PubMed: 18292570]
17. Gehring AJ, Dobos KM, Belisle JT, Harding CV, Boom WH. *Mycobacterium tuberculosis* LprG (Rv1411c): a novel TLR-2 ligand that inhibits human macrophage class II MHC antigen processing. *J Immunol.* 2004; 173:2660–8. [PubMed: 15294983]
18. Comas I, Chakravarti J, Small PM, Galagan J, Niemann S, Kremer K, et al. Human T cell epitopes of *Mycobacterium tuberculosis* are evolutionarily hyperconserved. *Nat Genet.* 2010; 42:498–503. [PubMed: 20495566]
19. Lopez M, Sly LM, Luu Y, Young D, Cooper H, Reiner NE. The 19-kDa *Mycobacterium tuberculosis* protein induces macrophage apoptosis through Toll-like receptor-2. *J Immunol.* 2003; 170:2409–16. [PubMed: 12594264]
20. Diaz-Silvestre H, Espinosa-Cueto P, Sanchez-Gonzalez A, Esparza-Ceron MA, Pereira-Suarez AL, Bernal-Fernandez G, et al. The 19-kDa antigen of *Mycobacterium tuberculosis* is a major adhesin that binds the mannose receptor of THP-1 monocytic cells and promotes phagocytosis of mycobacteria. *Microbial pathogenesis.* 2005; 39:97–107. [PubMed: 16098710]
21. Lancioni CL, Li Q, Thomas JJ, Ding X, Thiel B, Drage MG, et al. *Mycobacterium tuberculosis* lipoproteins directly regulate human memory CD4(+) T cell activation via Toll-like receptors 1 and 2. *Infect Immun.* 2011; 79:663–73. [PubMed: 21078852]
22. Gonzalez-Zamorano M, Mendoza-Hernandez G, Xolalpa W, Parada C, Vallecillo AJ, Bigi F, et al. *Mycobacterium tuberculosis* glycoproteomics based on ConA-lectin affinity capture of mannosylated proteins. *Journal of proteome research.* 2009; 8:721–33. [PubMed: 19196185]
23. Bigi, F.; Espitia, C.; Alito, A.; Zumarraga, M.; Romano, MI.; Cravero, S., et al. *Microbiology.* Vol. 143. Pt 11: 1997. A novel 27 kDa lipoprotein antigen from *Mycobacterium bovis*.; p. 3599-605.
24. Bigi F, Gioffre A, Klepp L, Santangelo MP, Alito A, Caimi K, et al. The knockout of the lprG-Rv1410 operon produces strong attenuation of *Mycobacterium tuberculosis*. *Microbes Infect.* 2004; 6:182–7. [PubMed: 14998516]
25. Drage MG, Tsai HC, Pecora ND, Cheng TY, Arida AR, Shukla S, et al. Mycobacterium tuberculosis lipoprotein LprG (Rv1411c) binds triacylated glycolipid agonists of Toll-like receptor 2. *Nat Struct Mol Biol.* 2010; 17:1088–95. [PubMed: 20694006]
26. Ocampo M, Patarroyo MA, Vanegas M, Alba MP, Patarroyo ME. Functional, biochemical and 3D studies of *Mycobacterium tuberculosis* protein peptides for an effective anti-tuberculosis vaccine. *Crit Rev Microbiol.* 2013
27. Ocampo M, Rodriguez DC, Rodriguez J, Bermudez M, Munoz CM, Patarroyo MA, et al. Rv1268c protein peptide inhibiting *Mycobacterium tuberculosis* H37Rv entry to target cells. *Bioorg Med Chem.* 2013
28. Patarroyo ME, Bermudez A, Patarroyo MA. Structural and immunological principles leading to chemically synthesized, multiantigenic, multistage, minimal subunit-based vaccine development. *Chem Rev.* 2011; 111:3459–507. [PubMed: 21438608]
29. Curtidor H, Vanegas M, Alba MP, Patarroyo ME. Functional, immunological and three-dimensional analysis of chemically synthesised sporozoite peptides as components of a fully-effective antimalarial vaccine. *Curr Med Chem.* 2011; 18:4470–502. [PubMed: 22029724]
30. Rodriguez LE, Curtidor H, Urquiza M, Cifuentes G, Reyes C, Patarroyo ME. Intimate molecular interactions of *P. falciparum* merozoite proteins involved in invasion of red blood cells and their implications for vaccine design. *Chem Rev.* 2008; 108:3656–705. [PubMed: 18710292]
31. Acosta A, Norazmi MN, Hernandez-Pando R, Alvarez N, Borrero R, Infante JF, et al. The importance of animal models in tuberculosis vaccine development. *Malays J Med Sci.* 2011; 18:5–12. [PubMed: 22589668]
32. Kolibab K, Parra M, Yang AL, Perera LP, Derrick SC, Morris SL. A practical *in vitro* growth inhibition assay for the evaluation of TB vaccines. *Vaccine.* 2009; 28:317–22. [PubMed: 19879231]
33. Parra M, Yang AL, Lim J, Kolibab K, Derrick S, Cadieux N, et al. Development of a murine mycobacterial growth inhibition assay for evaluating vaccines against *Mycobacterium tuberculosis*. *Clin Vaccine Immunol.* 2009; 16:1025–32. [PubMed: 19458207]

34. Restrepo-Montoya D, Vizcaino C, Nino LF, Ocampo M, Patarroyo ME, Patarroyo MA. Validating subcellular localization prediction tools with mycobacterial proteins. *BMC Bioinformatics*. 2009; 10:134. [PubMed: 19422713]
35. Vizcaino C, Restrepo-Montoya D, Rodriguez D, Nino LF, Ocampo M, Vanegas M, et al. Computational prediction and experimental assessment of secreted/surface proteins from *Mycobacterium tuberculosis* H37Rv. *PLoS Comput Biol*. 2010; 6:e1000824. [PubMed: 20585611]
36. Larsen JE, Lund O, Nielsen M. Improved method for predicting linear B-cell epitopes. *Immunome research*. 2006; 2:2. [PubMed: 16635264]
37. Kyhse-Andersen J. Electrophoretic transfer of proteins from polyacrylamide to nitrocellulose: a simple apparatus without buffer tank for rapid transfer of proteins from polyacrylamide to nitrocellulose. *Journal of biochemical and biophysical methods*. 1984; 10:203–9. [PubMed: 6530509]
38. Sreerama N, Venyaminov SY, Woody RW. Estimation of the number of alpha-helical and beta-strand segments in proteins using circular dichroism spectroscopy. *Protein Sci*. 1999; 8:370–80. [PubMed: 10048330]
39. Bermudez LE, Goodman J. *Mycobacterium tuberculosis* invades and replicates within type II alveolar cells. *Infect Immun*. 1996; 64:1400–6. [PubMed: 8606107]
40. Chapeton-Montes JA, Plaza DF, Barrero CA, Patarroyo MA. Quantitative flow cytometric monitoring of invasion of epithelial cells by *Mycobacterium tuberculosis*. *Front Biosci*. 2008; 13:650–6. [PubMed: 17981577]
41. El-Shazly S, Ahmad S, Mustafa AS, Al-Attayah R, Krajci D. Internalization by HeLa cells of latex beads coated with mammalian cell entry (Mce) proteins encoded by the mce3 operon of *Mycobacterium tuberculosis*. *Journal of medical microbiology*. 2007; 56:1145–51. [PubMed: 17761475]
42. Noss EH, Harding CV, Boom WH. *Mycobacterium tuberculosis* inhibits MHC class II antigen processing in murine bone marrow macrophages. *Cell Immunol*. 2000; 201:63–74. [PubMed: 10805975]
43. Pai RK, Convery M, Hamilton TA, Boom WH, Harding CV. Inhibition of IFN-gamma-induced class II transactivator expression by a 19-kDa lipoprotein from *Mycobacterium tuberculosis*: a potential mechanism for immune evasion. *J Immunol*. 2003; 171:175–84. [PubMed: 12816996]
44. Chitale S, Ehrt S, Kawamura I, Fujimura T, Shimono N, Anand N, et al. Recombinant *Mycobacterium tuberculosis* protein associated with mammalian cell entry. *Cell Microbiol*. 2001; 3:247–54. [PubMed: 11298648]
45. Sreerama N, Woody RW. Estimation of protein secondary structure from circular dichroism spectra: comparison of CONTIN, SELCON, and CDSSTR methods with an expanded reference set. *Anal Biochem*. 2000; 287:252–60. [PubMed: 11112271]
46. Wolfe LM, Mahaffey SB, Kruh NA, Dobos KM. Proteomic definition of the cell wall of *Mycobacterium tuberculosis*. *J Proteome Res*. 2010; 9:5816–26. [PubMed: 20825248]
47. Patarroyo MA, Bermudez A, Lopez C, Yepes G, Patarroyo ME. 3D analysis of the TCR/pMHCII complex formation in monkeys vaccinated with the first peptide inducing sterilizing immunity against human malaria. *PLoS One*. 2010; 5:e9771. [PubMed: 20333301]
48. Karosiene E, Rasmussen M, Blicher T, Lund O, Buus S, Nielsen M. NetMHCIIpan-3.0, a common pan-specific MHC class II prediction method including all three human MHC class II isotypes, HLA-DR, HLA-DP and HLA-DQ. *Immunogenetics*. 2013; 65:711–24. [PubMed: 23900783]

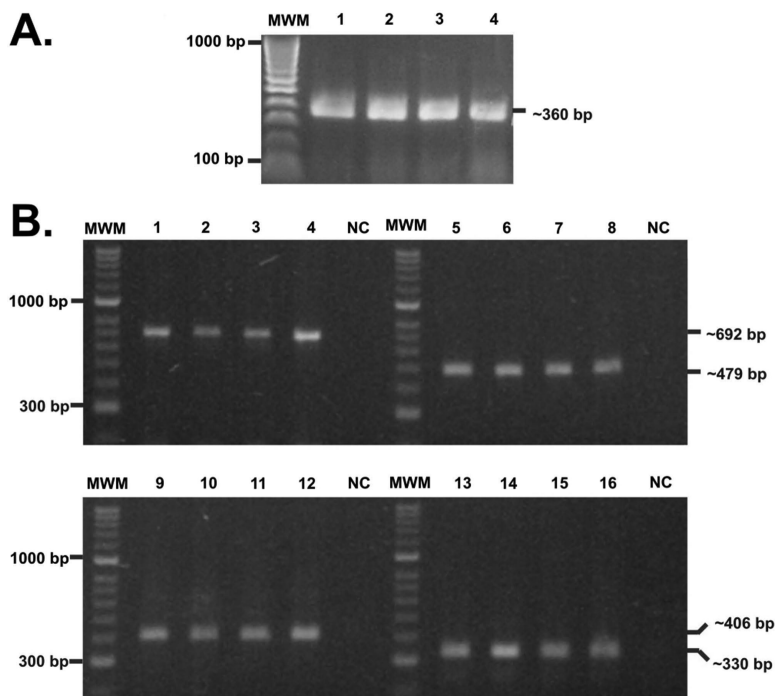


Figure 1.

Assessing *rv1411c*, *rv1911c*, *rv2270* and *rv3763* genes presence. **(A)** Amplification of the *rpoB* gene from gDNA isolated from the species and strains included in this study. MWM: molecular weight marker (1 kb); 1. *M. tuberculosis* H37Rv; 2. *M. tuberculosis* H37Ra; 3. *M. bovis*; 4. *M. bovis* BCG.

(B) PCR amplification of gDNA isolated from the mycobacterial species and strains evaluated here. MWM: molecular weight marker (1 kb); Lanes 1-4 show *rv1411* gene presence in: (1) *M. tuberculosis* H37Rv, (2) *M. tuberculosis* H37Ra, (3) *M. bovis*, (4) and *M. bovis* BCG; Lanes 5-8 show *rv1911* gene presence in: (5) *M. tuberculosis* H37Rv, (6) *M. tuberculosis* H37Ra, (7) *M. bovis* and (8) *M. bovis* BCG. Lanes 9-12 show *rv2270* gene presence in: (9) *M. tuberculosis* H37Rv, (10) *M. tuberculosis* H37Ra, (11) *M. bovis* and (12) *M. bovis* BCG; Lanes 13-16 show *rv3763* gene presence in: (13) *M. tuberculosis* H37Rv, (14) *M. tuberculosis* H37Ra, (15) *M. bovis* and (16) *M. bovis* BCG. NC. Negative PCR control.

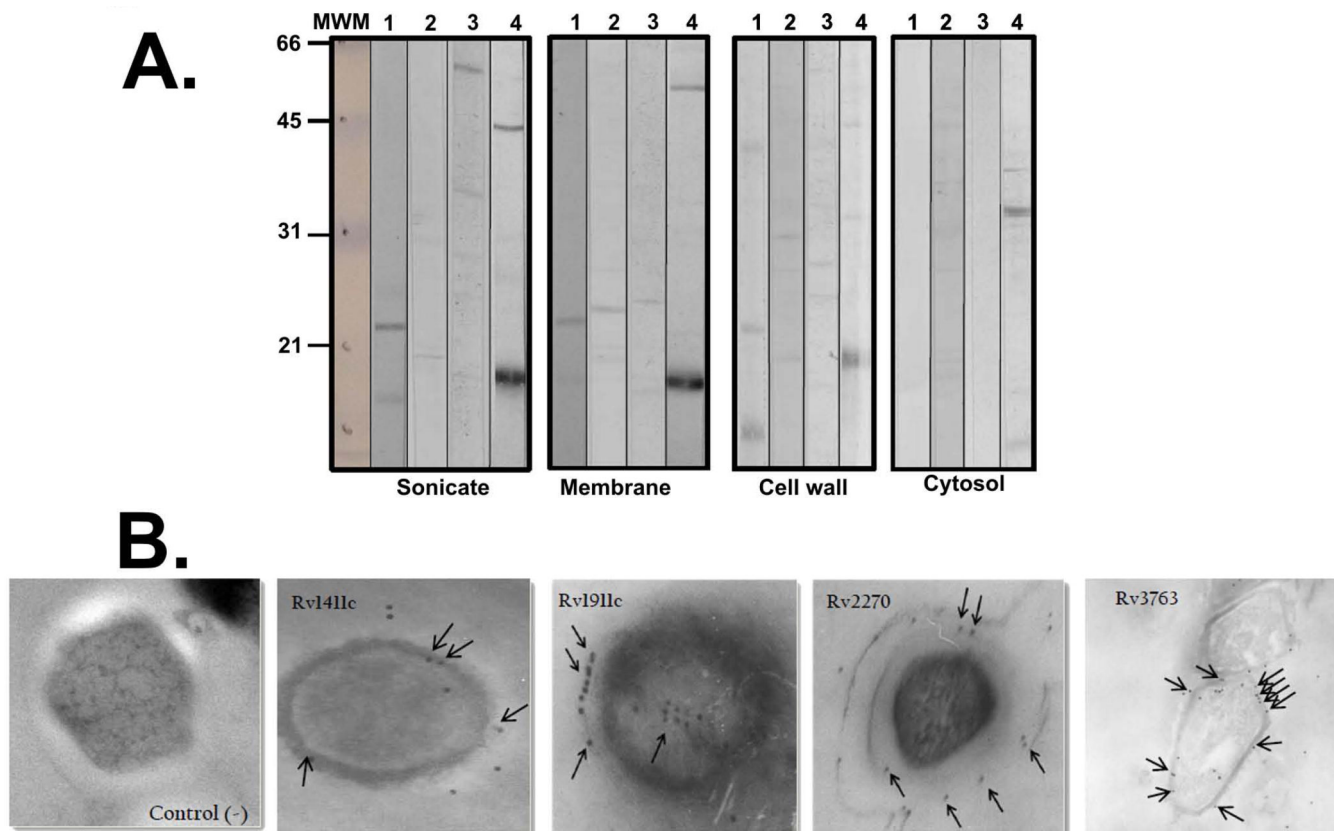


Figure 2. Lipoprotein recognition. **(A)** Western blot with rabbit pre-immune serum and post-third inoculation against *M. tuberculosis* H37Rv total sonicat and subcellular fractions (membrane, cell wall and cytosol). Lanes 1 to 4 show post-third immune serum. Serums were obtained by inoculating polymeric peptides, as mentioned in the Materials and Methods section: (1) Rv1411c; (2) Rv1911c; (3) Rv2270 and (4) Rv3763. The molecular weight marker is shown on the left-hand side of the Figure. **(B)** Immunoelectron microscopy. 6,000 x magnification. Lipoprotein detection can be seen on *M. tuberculosis* H37Rv bacillus surface, as indicated by the colloidal gold particles indicated by black arrows.

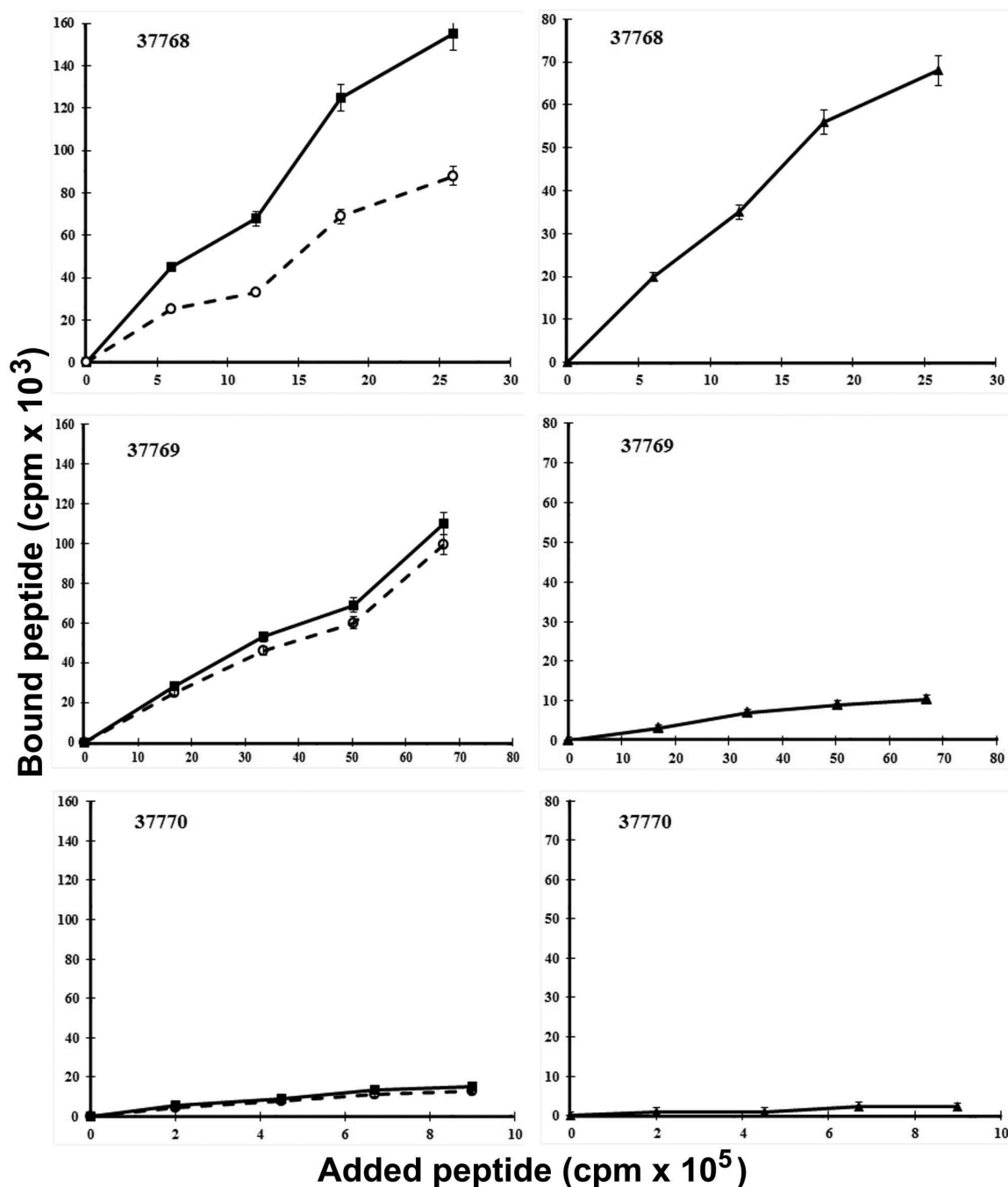


Figure 3.

Cell binding assay patterns. Graph lines to the left show: (■) total binding; cells plus radio-labelled peptide, (○) non-specific binding; cells, radio-labelled peptide and excess unlabelled peptide representing residual radio-labelled peptide bound with added 400x concentration of identical unlabelled peptide, (▲) specific binding = [total binding - non-specific binding]. The upper panel shows a strongly bound peptide (e.g. 37768), the central panel shows a non-specific binding peptide (e.g. 37769) and the lower panel a A549 cell binding peptide having low binding activity (e.g., 37770).

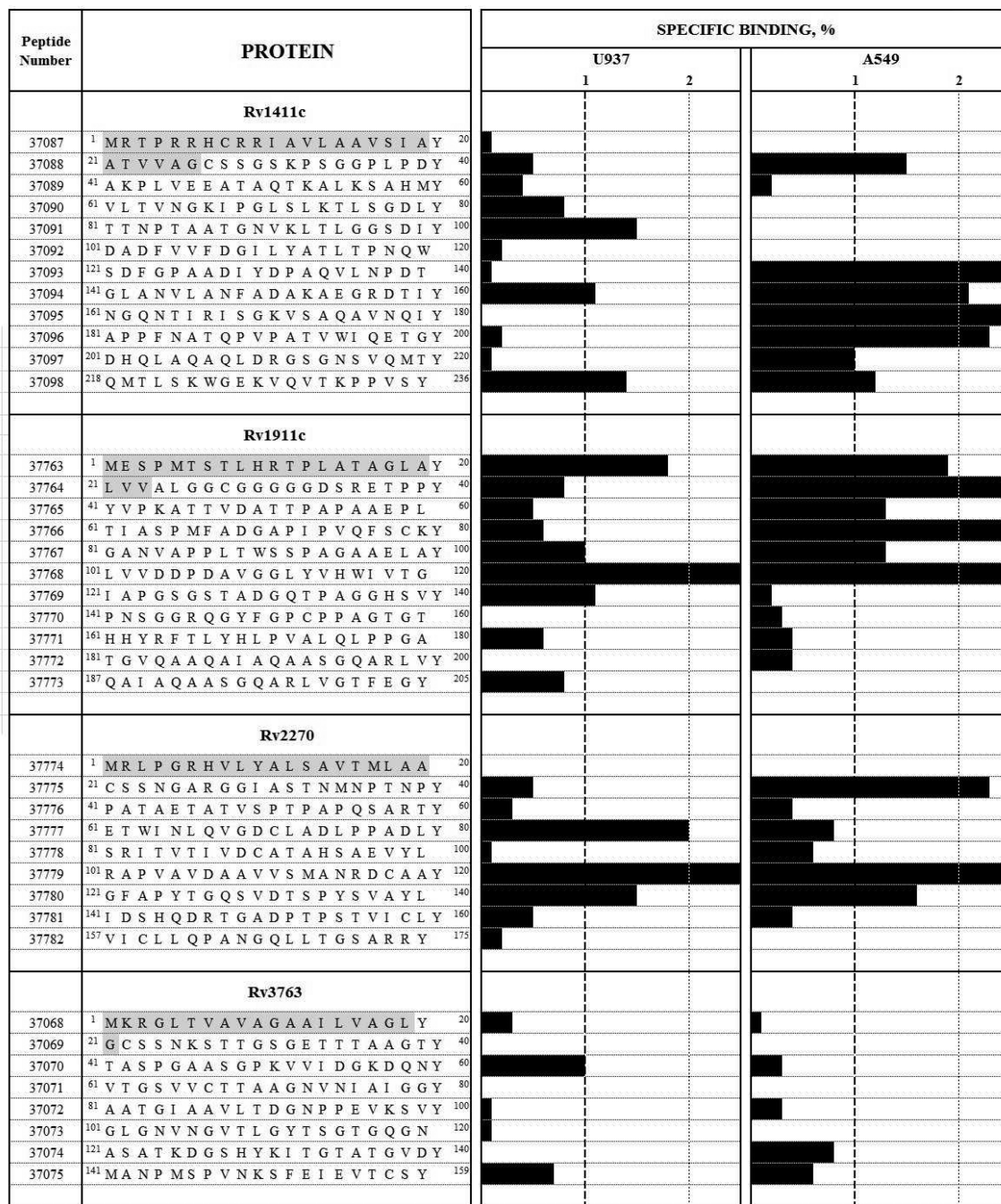


Figure 4. Receptor-ligand assays. A549 and U937 cell binding profiles for Rv1411c, Rv1911c, Rv2270 and Rv3763 synthetic peptides. The institute's synthetic peptide serial numbers and amino acid sequences are shown on the left of the Figure. Horizontal black bars represent specific binding capacity, expressed as percentages for each peptide in both cell lines tested here. Vertical dotted lines show the 1% specific binding cut-off above which a peptide was considered to be a HABP. Signal amino acid sequences are shown in grey.

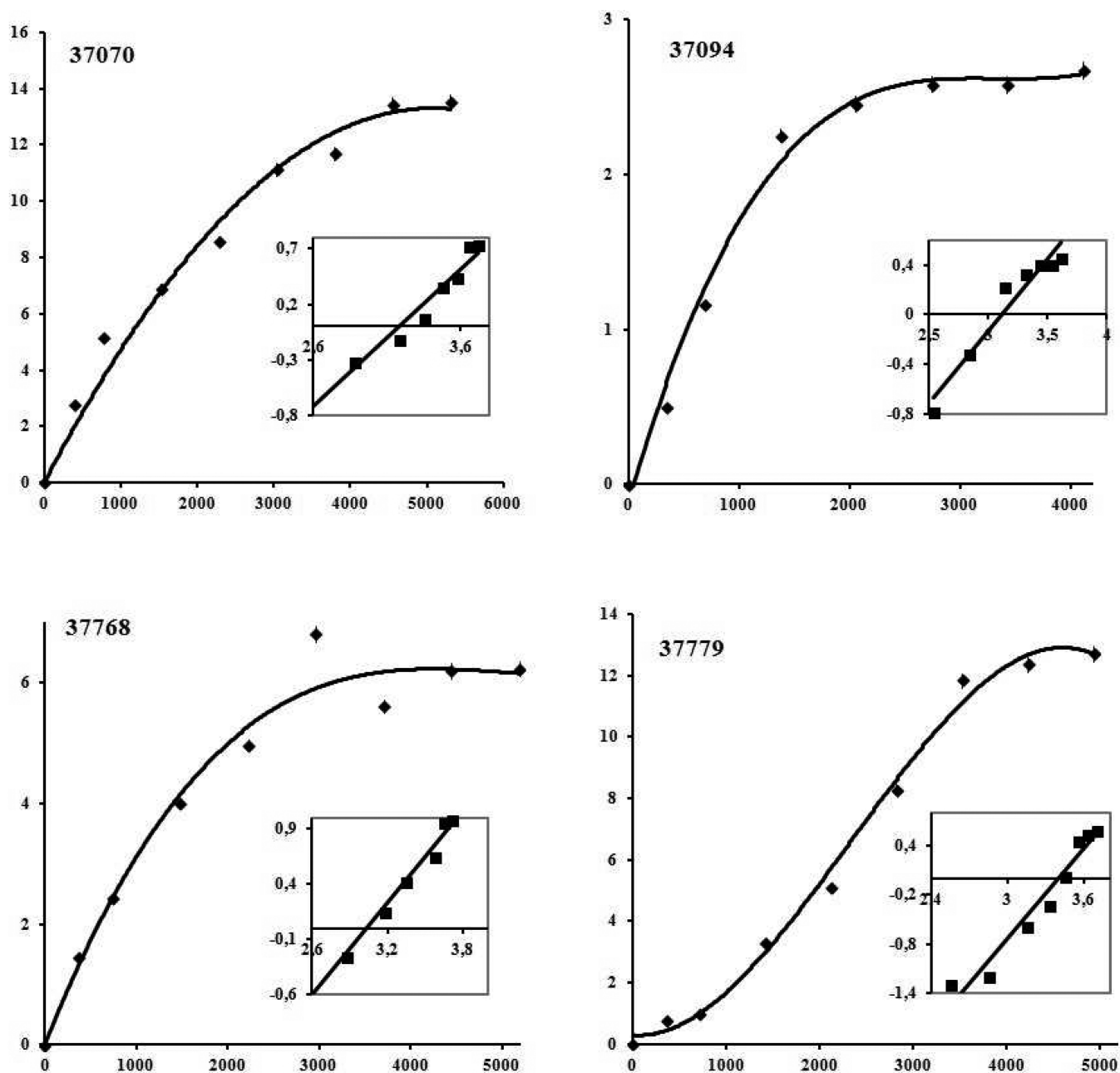


Figure 5. Saturation curves for HABPs 37070, 37094, 37768 and 37779 which bound with high activity to U937 cells. Saturation curves were obtained by plotting the amount of specifically bound ^{125}I -HABP against the amount of free ^{125}I -HABP. Affinity constants and the maximum number of sites per cell were obtained from these curves by Hill analysis. Inset: the abscissa is $\text{Log } F$ in the Hill Plot and the ordinate is $\text{Log}[B/B_{\text{max}} - B]$, B_{max} being the maximum amount of bound peptide, B the bound peptide and F the free peptide.

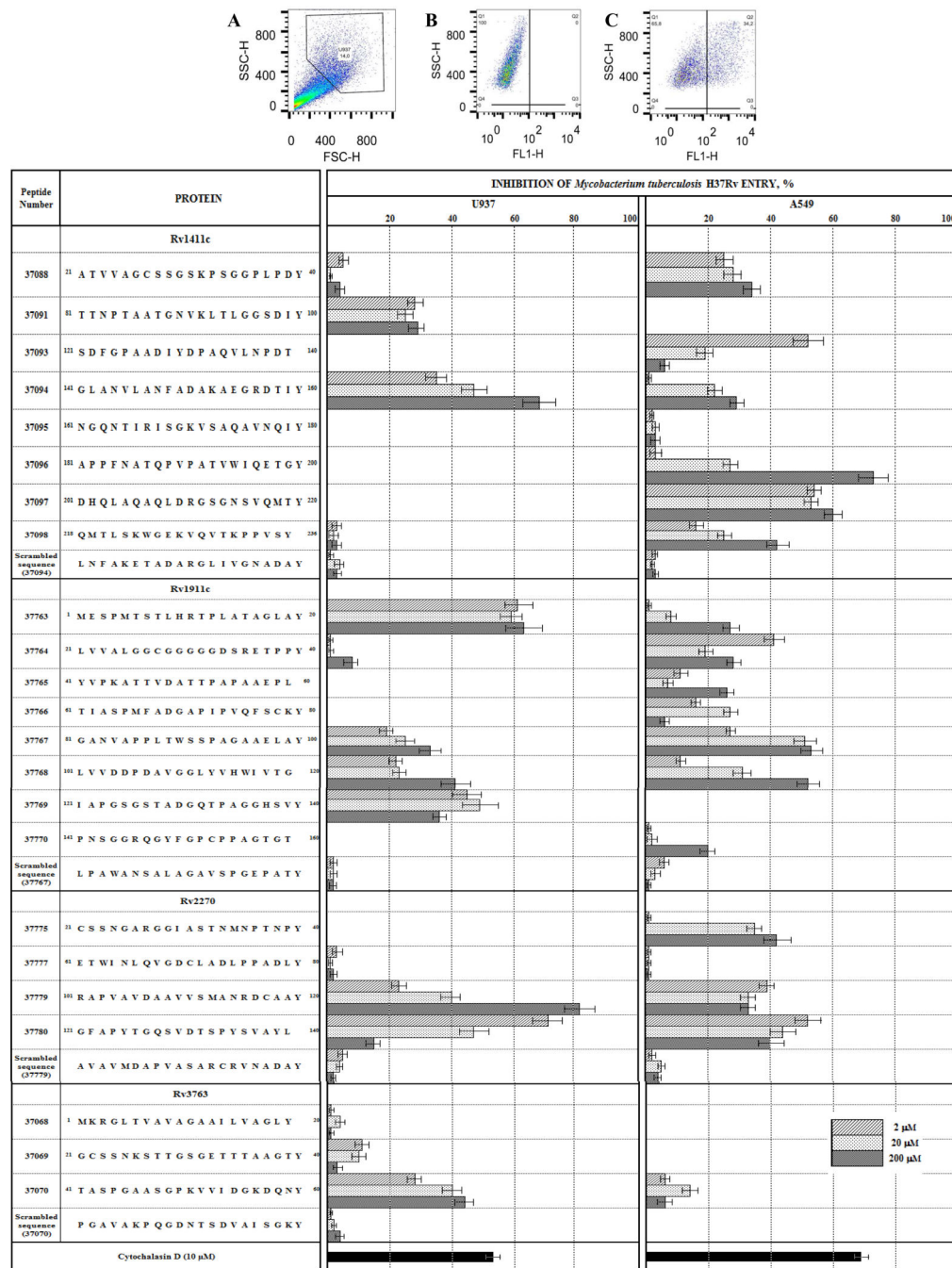


Figure 6. HABP inhibition ability. The upper panel shows the density plots for invasion assay for a selected cell population (A) in HABP presence (inhibition) (B) or absence (non-inhibition) (C). 10 μM cytochalasin was used as positive invasion inhibition control in both cases. The bottom panel shows the inhibitions entry to mycobacterial target. The institute's synthetic peptide serial numbers and amino acid sequences are shown on the left of the Figure. Horizontal black bars represent percentages of mycobacterial invasion into A549 and U937

cell lines at different peptide concentrations. The results correspond to the percentage of invasion inhibition, calculated for each treatment \pm standard deviation.

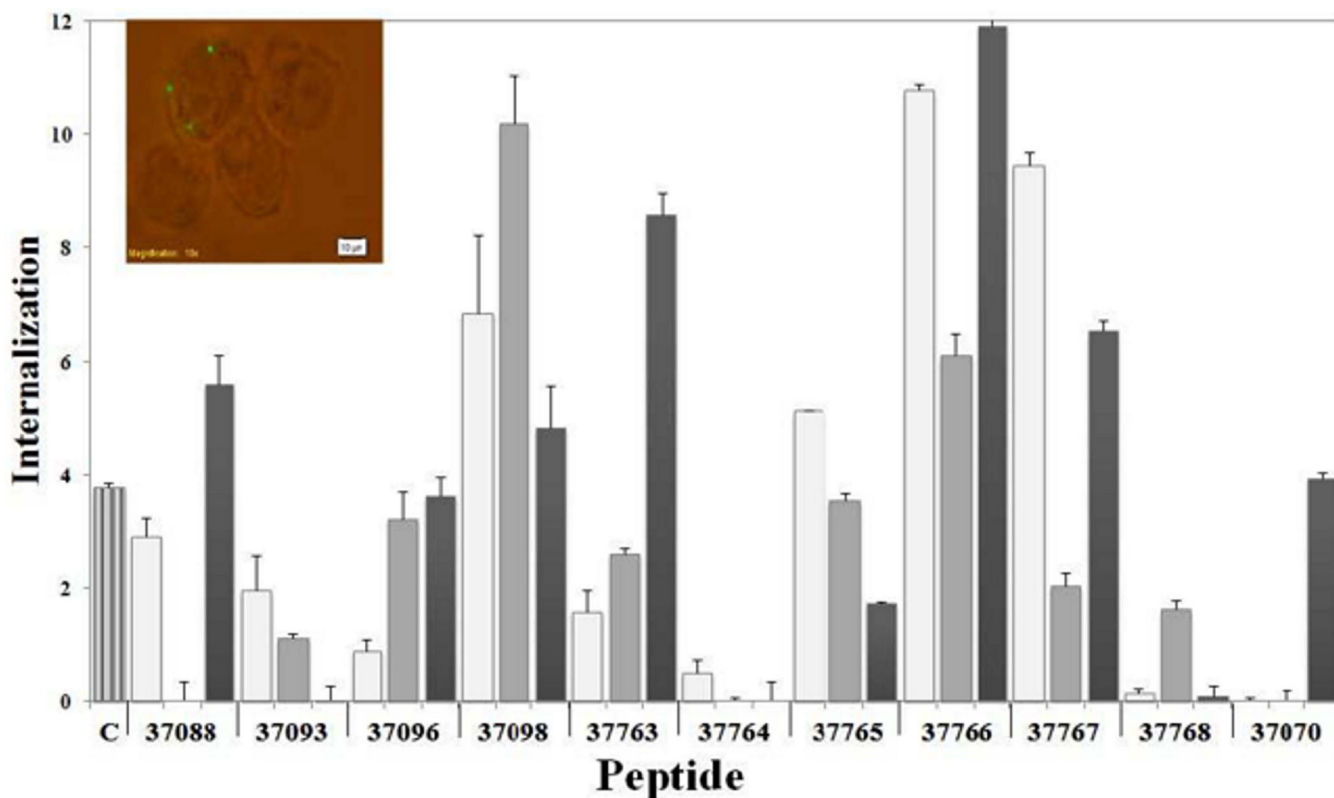


Figure 7. Percentages of peptide-coated microspheres internalised by A549 cells. A549 cells were independently incubated with peptides and then with uncoated microspheres as control treatment (subtracted from the final result for each peptide). Untreated microspheres were used as negative control (C). The results were the average internalisation calculated for each treatment \pm SD. * $p < 0.01$; ** $p < 0.001$, according to a two-tailed Student's *t*-test. Insert shows the fluorescence microscopy of latex beads internalised by A549 cells.